



Adaptation of light-harvesting functions of unicellular green algae to different light qualities

Yoshifumi Ueno¹ · Shimpei Aikawa² · Akihiko Kondo³ · Seiji Akimoto¹

Received: 13 March 2018 / Accepted: 20 May 2018 / Published online: 28 May 2018
© Springer Science+Business Media B.V., part of Springer Nature 2018

Abstract

Oxygenic photosynthetic organisms perform photosynthesis efficiently by distributing captured light energy to photosystems (PSs) at an appropriate balance. Maintaining photosynthetic efficiency under changing light conditions requires modification of light-harvesting and energy-transfer processes. In the current study, we examined how green algae regulate their light-harvesting functions in response to different light qualities. We measured low-temperature time-resolved fluorescence spectra of unicellular green algae *Chlamydomonas reinhardtii* and *Chlorella variabilis* cells grown under different light qualities. By observing the delayed fluorescence spectra, we demonstrated that both types of green algae primarily modified the associations between light-harvesting chlorophyll protein complexes (LHCs) and PSs (PSII and PSI). Under blue light, *Chlamydomonas* transferred more energy from LHC to chlorophyll (Chl) located far from the PSII reaction center, while energy was transferred from LHC to PSI via different energy-transfer pathways in *Chlorella*. Under green light, both green algae exhibited enhanced energy transfer from LHCs to both PSs. Red light induced fluorescence quenching within PSs in *Chlamydomonas* and LHCs in *Chlorella*. In *Chlorella*, energy transfer from PSII to PSI appears to play an important role in balancing excitation between PSII and PSI.

Keywords Light harvesting · Energy transfer · Light adaptation · Green algae · Photosystem

Abbreviations

Car	Carotenoid
Chl	Chlorophyll
DF	Delayed fluorescence
FDAS	Fluorescence decay-associated spectrum (spectra)
LED	Light-emitting diodes
LHC	Light-harvesting chlorophyll protein complex
LHCSR	Light-harvesting complex stress-related
PBS	Phycobilisome
PC	Phycocyanin
PE	Phycoerythrin
PS	Photosystem

RC	Reaction center
TRFS	Time-resolved fluorescence spectrum (spectra)

Introduction

Oxygenic photosynthetic organisms capture light energy via light-harvesting antennas, and convert it to electron flow in the reaction center (RC) of photosystems (PSs). Because electron transfer is shared between two PSs (PSII and PSI) via the cytochrome *b₆/f* complex, the preservation of excitation balance between PSII and PSI is extremely important for ensuring efficient photosynthesis (Blankenship 2014; Mirkovic et al. 2017). Oxygenic photosynthetic organisms expand the available wavelength of light via specific light-harvesting antennas. Cyanobacteria and red algae contain large light-harvesting antennas called phycobilisomes (PBSs), which absorb visible light and comprise an allophycocyanin core surrounded by rods containing phycocyanin (PC) only or a combination of phycoerythrin (PE) with PC (Gantt 1981). Green algae and land plants possess a light-harvesting chlorophyll (Chl) protein complex (LHC) which contains Chl *a*, Chl *b*, and carotenoid (Car) (Liu et al. 2004).

✉ Seiji Akimoto
akimoto@hawk.kobe-u.ac.jp

¹ Graduate School of Science, Kobe University,
Kobe 657-8501, Japan

² Japan International Research Center for Agricultural
Sciences, Tsukuba 305-8686, Japan

³ Graduate School of Science, Technology and Innovation,
Kobe University, Kobe 657-8501, Japan

Photosynthetic organisms regulate the quantity and/or quality of pigment–protein complexes and interactions among the pigment–protein complexes in response to changing light conditions. The regulatory mechanisms for specific light qualities have been studied for some photosynthetic organisms (Ghosh and Govindjee 1966; Ley and Butler 1980; Myers et al. 1980; Melis and Harvey 1981; Kowallik and Schürmann 1984; Manodori and Melis 1986; Humbeck et al. 1988; Chow et al. 1990; Cunningham et al. 1990; Aizawa et al. 1992; Melis et al. 1996; Murakami 1997; Chen et al. 2010; Akimoto et al. 2012, 2013; Markou 2014; Ueno et al. 2015).

The PC/Chl *a* ratio in the cyanobacterium *Synechococcus* sp. PCC 6301 is reported to be reduced under light that excites PSII (yellow and orange lights) and increased under red light, which excites PSI (Ghosh and Govindjee 1966; Myers et al. 1980; Manodori and Melis 1986). The cyanobacterium *Arthrospira platensis* grown under light that PBS does not absorb (blue and far-red lights) was found to exhibit an increased PC/Chl *a* ratio (Chen et al. 2010; Akimoto et al. 2012; Markou 2014). Red alga *Porphyridium cruentum* was found to exhibit decreased and increased PE/Chl *a* ratio under green- and red-light cultivation, respectively (Ley and Butler 1980; Cunningham et al. 1990). Red alga *Cyanidioschyzon merolae*, whose pigment composition is similar to that of typical cyanobacteria due to a lack of PE, exhibited a reduced PC/Chl *a* ratio under yellow and red light, whereas the opposite response was observed under blue and green light (Ueno et al. 2015). Unicellular green algae *Chlorella vulgaris*, *Scenedesmus obliquus*, and *Chlamydomonas reinhardtii* (hereafter, *Chlamydomonas*) grown under red light exhibited an increased Chl *a*/Chl *b* ratio (Kowallik and Schürmann 1984; Humbeck et al. 1988; Melis et al. 1996), while land plant *Pisum sativum* L. showed the opposite response (Melis and Harvey 1981; Chow et al. 1990). In cyanobacteria and red algae, the PSI/PSII ratio was found to increase and decrease under light that excites PSII (green, yellow, and orange lights) and PSI (red light), respectively (Myers et al. 1980; Manodori and Melis 1986; Cunningham et al. 1990; Aizawa et al. 1992; Murakami 1997). Green algae and land plants induced lower PSI/PSII ratios under red light compared with light that excites PSII (Melis and Harvey 1981; Chow et al. 1990; Melis et al. 1996; Murakami 1997).

Not only the alteration of pigment and protein composition but also the regulation of energy distribution may occur for a long-term adaptation. Previously, we investigated the excitation energy-transfer processes of *A. platensis* and *C. merolae* grown under light with different qualities (Akimoto et al. 2012, 2013; Ueno et al. 2015). *A. platensis* regulated both the energy transfer from PBS to PSI and that from PSII to PSI (spillover) to balance excitation between both PSs (Akimoto et al. 2013). In *C. merolae*, energy-transfer

processes to PSI were sensitive to yellow and red light; yellow light promoted both the energy transfer from PBS to PSI and from PSII to PSI, while red light suppressed the spillover (Ueno et al. 2015). However, in the case of green algae, the relationship between light qualities and energy-transfer processes is poorly understood for a long-term adaptation. In the present study, we examined how green algae modify their light-harvesting and energy-transfer processes under different light qualities. We measured steady-state absorption spectra, steady-state fluorescence spectra with absolute intensity, and time-resolved fluorescence spectra (TRFS) at 77 K of unicellular green algae *Chlamydomonas* and *Chlorella variabilis* (hereafter, *Chlorella*) cells grown under white (W) and monochromatic (blue [B], green [G], and red [R]) light-emitting diodes (LEDs). Moreover, by combining absolute steady-state fluorescence spectra and TRFS, we constructed fluorescence decay-associated spectra (FDAS) with absolute amplitude.

Materials and methods

Cultivation conditions

Chlamydomonas and *Chlorella* cells were cultured at 25 °C with 100 rpm agitation under 50 $\mu\text{mol photons m}^{-2} \text{s}^{-1}$ continuous illumination by W-LED in air in 250-mL Erlenmeyer flasks containing 100 mL liquid medium. The cultured cells were repeatedly inoculated into fresh medium, liquid high-salt medium (Sueoka 1960) (*Chlamydomonas*), and C medium (Ichimura 1971) supplemented with 20 mM serine (*Chlorella*), at an optical density of 750 nm (OD_{750}) = 0.04 at 7-day intervals. Cells inoculated in fresh medium were then transferred and cultivated under different light qualities (50 $\mu\text{mol photons m}^{-2} \text{s}^{-1}$ continuous illumination). Cells cultivated for 6 days were used for measurements. We used cells grown under W-LED as a control. The spectral profiles of LEDs used for cultivation and absorption spectra of the control cells at 77 K are presented in Fig. 1. The B-, G-, and R-LEDs peaked at 477, 514, and 666 nm, respectively. The cellular absorption spectra indicated that B-LED was absorbed by Chl *b* (Soret) and Car, G-LED was absorbed by Car, and R-LED was absorbed mainly by Chl *a* (Qy) and slightly by Chl *b* (Qy).

Measurements and analyses

Steady-state absorption spectra were measured using a spectrometer equipped with an integrating sphere at 77 K (JASCO V-650/ISVC-747; Ueno et al. 2015). Steady-state fluorescence spectra with an absolute intensity of 77 K were measured with a spectrofluorometer equipped with an integrating sphere (JASCO FP-6600/ILFC-543L; Ueno et al. 2018). The

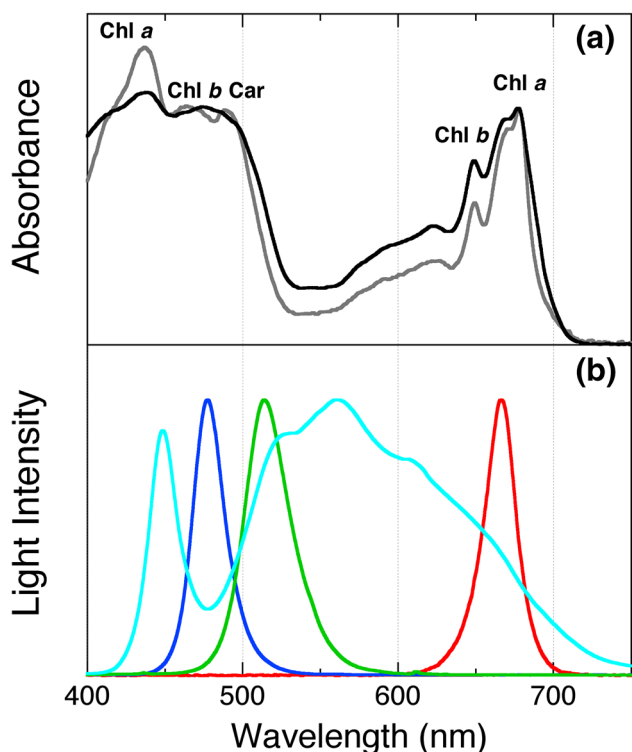


Fig. 1 Absorption spectra of *Chlamydomonas* (black line) and *Chlorella* (gray line) cells grown under white LEDs (*Car* carotenoid, *Chl* chlorophyll) (a), and emission spectra of white LEDs (cyan line), blue LEDs (blue line), green LEDs (green line), and red LEDs (red line) (b)

excitation wavelength was 460 nm, resulting in LHC excitation. TRFS were measured from 660 to 750 nm at 1-nm intervals using a time-correlated single-photon counting system at 77 K (Akimoto et al. 2012). The excitation wavelength was 459 nm. The repetition rate of the pulse train was 3 MHz. The time interval for data acquisition was set to 2.4 or 24.4 ps/channel (total time window = 10 or 100 ns, respectively). For steady-state and time-resolved fluorescence measurements, homogenous ice was obtained by adding polyethylene glycol (average molecular weight 3350, final concentration 15% [w/v], Sigma-Aldrich, St Louis, MO, USA) to a sample solution at 77 K (final OD₆₈₀ = 1.5). Obtained fluorescence spectra were corrected using a substandard lamp with a known profile. The measured fluorescence rise and decay curves from three biological replicates were summed and fitted globally by sums of exponentials with common time constants, as follows:

$$F(t, \lambda) = \sum_{n=1}^6 A_n(\lambda) \exp\left(-\frac{t}{\tau_n}\right), \tag{1}$$

where $A_n(\lambda)$ is the amplitude at different detection wavelengths and τ_n is the time constant. The amplitudes of these

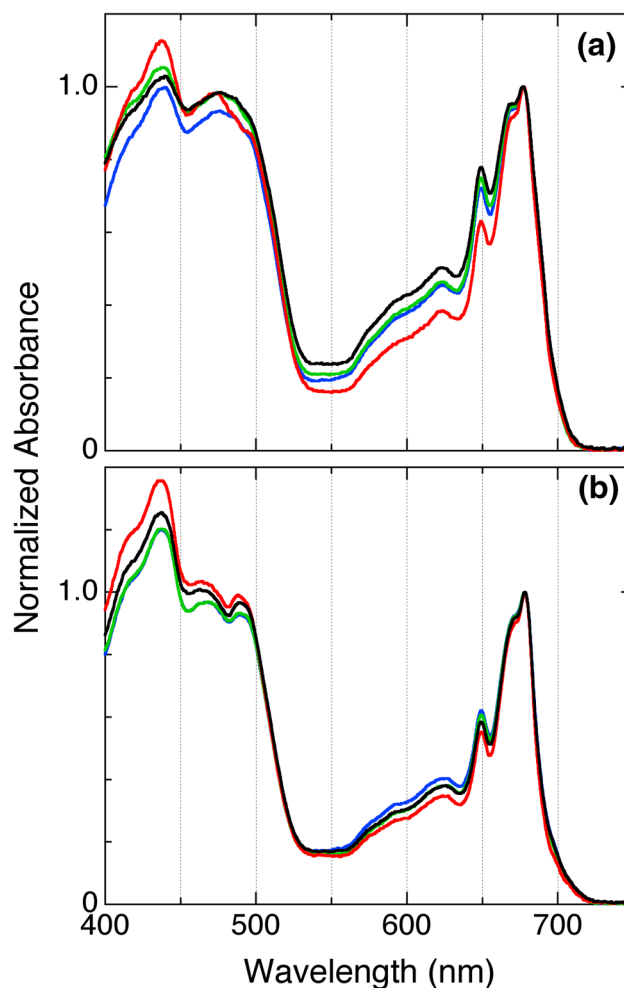


Fig. 2 Steady-state absorption spectra of *Chlamydomonas* (a) and *Chlorella* (b) cells grown under different light qualities at 77 K. The spectra are normalized by the *Chl a* Qy band. The black, blue, green, and red lines indicate the cells grown under white, blue, green, and red LEDs, respectively. The spectra are averages of three different biological replicates

exponential components as a function of emission wavelength provided FDAS.

Results

Steady-state absorption spectra

Figure 2 shows the steady-state absorption spectra at 77 K of *Chlamydomonas* and *Chlorella* cells grown under different light qualities. All spectra were normalized by the *Chl a* Qy band. *Chl a* exhibited the Soret band (~440 nm) and the Qy band (~680 nm), while *Chl b* exhibited absorption peaks at ~470 and ~650 nm, corresponding to the Soret band and the Qy band, respectively. The peak at ~490 nm was assigned to *Car*. The peak at ~470 nm exhibited not only

Chl *b* absorption but also Car absorption. Two absorption peaks at ~470 nm and ~490 nm were found in *Chlorella*, while these peaks formed one band in *Chlamydomonas*. The Chl *b*/Chl *a* ratio was larger in *Chlamydomonas* than in *Chlorella* (Table 1). Compared with the W-grown cells, the light quality affected the relative Car and Chl *b* content and growth (OD₇₅₀) (see Table 1). In *Chlamydomonas*, the Chl *b*/Chl *a* ratio decreased under R-LED and the ratio was slightly reduced under B- and G-LED conditions. The Car/Chl *a* ratio also decreased under B- and R-LED conditions. For *Chlorella*, the Chl *b*/Chl *a* ratio was reduced under R-LED like *Chlamydomonas*, while the ratio slightly increased under B- and G-LED conditions. The cell growth of *Chlamydomonas* was reduced, but that of *Chlorella* did not change under monochromatic LEDs.

Steady-state fluorescence spectra

To examine the energy distribution from LHC to both PSs, we measured low-temperature steady-state fluorescence spectra on LHC-selective excitation. Figure 3 shows steady-state fluorescence spectra of *Chlamydomonas* and *Chlorella* with 460-nm excitation. The spectra were normalized to the intensity of excitation light absorbed into samples. The spectra were divided into two fluorescence regions: PSII (≤ 700 nm) and PSI (≥ 700 nm). Two fluorescence bands below 700 nm have been reported to originate from CP43 (~685 nm) and CP47 (~695 nm) in PSII (Andrizhiyevskaya et al. 2005; Shibata et al. 2013), while a maximum above 700 nm is reported to derive from red-Chl in PSI (Garnier et al. 1986; Ihalainen et al. 2005). PSI fluorescence band at ~714 nm was observed in

Table 1 Relative intensities of the carotenoid band (~490 nm) and the chlorophyll (Chl) *b* Qy band (~650 nm) to the Chl *a* Qy band (~678 nm) in the absorption spectra and optical density at 750 nm (OD₇₅₀) of *Chlamydomonas* and *Chlorella* cells grown under different light qualities

Sample	Relative intensities		OD ₇₅₀
	Car/Chl <i>a</i>	Chl <i>b</i> /Chl <i>a</i>	
<i>C. reinhardtii</i>			
White	0.95 ± 0.01	0.78 ± 0.02	0.639 ± 0.003
Blue	0.89 ± 0.01	0.72 ± 0.02	0.385 ± 0.007
Green	0.94 ± 0.01	0.75 ± 0.01	0.421 ± 0.017
Red	0.89 ± 0.01	0.63 ± 0.01	0.321 ± 0.004
<i>C. variabilis</i>			
White	0.97 ± 0.01	0.58 ± 0.01	0.810 ± 0.003
Blue	0.93 ± 0.01	0.62 ± 0.00	0.777 ± 0.003
Green	0.93 ± 0.01	0.61 ± 0.01	0.803 ± 0.003
Red	0.98 ± 0.01	0.55 ± 0.00	0.793 ± 0.021

OD₇₅₀ after 6 days of cultivation is shown. All values are the means ± SDs of three biological replicates

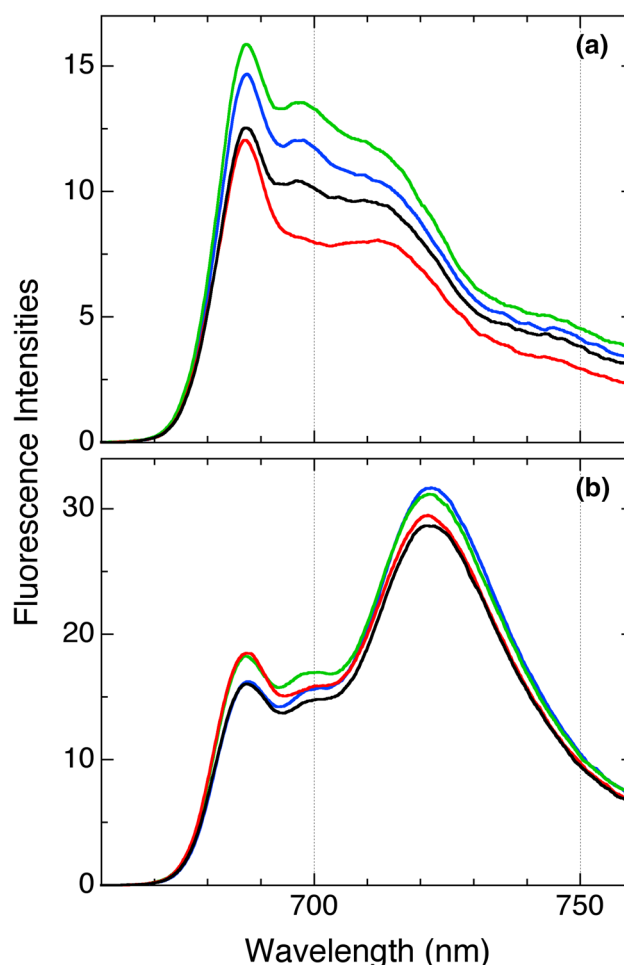


Fig. 3 Steady-state fluorescence spectra of *Chlamydomonas* (a) and *Chlorella* (b) cells grown under different light qualities at 77 K. The excitation wavelength was set to 460 nm. The spectra are normalized to the intensity of the excitation light absorbed by the sample. The black, blue, green, and red lines indicate the cells grown under white, blue, green, and red LEDs, respectively. The spectra are averages of three different biological replicates

Chlamydomonas, while a clear peak at ~722 nm was found in *Chlorella*, indicating that *Chlorella* exhibited lower-energy red-Chl compared with *Chlamydomonas*. Absolute fluorescence intensities of CP43, CP47, and PSI are summarized in Table 2. For *Chlamydomonas*, all fluorescence bands increased under G-LED, PSII bands increased under B-LED, and fluorescence bands except CP43 were reduced under R-LED. For *Chlorella*, all fluorescence bands increased under G-LED like *Chlamydomonas*. However, the effects of B- and R-LED conditions were different from those in *Chlamydomonas*: all fluorescence bands except CP43 increased under B-LED, while PSII bands became larger under R-LED in *Chlorella*.

Table 2 Fluorescence intensities of CP43, CP47, and PSI in *Chlamydomonas* and *Chlorella* cells grown under different light qualities

Sample	CP43	CP47	PSI
<i>C. reinhardtii</i>			
White	12.5 ± 0.6	10.4 ± 0.3	6.90 ± 0.34
Blue	14.6 ± 0.9	12.1 ± 1.0	7.27 ± 0.54
Green	15.9 ± 1.0	13.5 ± 0.2	8.22 ± 0.28
Red	12.0 ± 0.0	8.13 ± 0.03	5.52 ± 0.16
<i>C. variabilis</i>			
White	16.0 ± 0.4	14.7 ± 0.6	25.4 ± 0.9
Blue	16.2 ± 0.2	15.6 ± 0.1	28.5 ± 0.8
Green	18.2 ± 1.3	17.0 ± 1.1	27.5 ± 1.5
Red	18.5 ± 1.1	15.7 ± 0.8	25.7 ± 0.6

The wavelengths of CP43, CP47, and PSI in *Chlamydomonas* were 687, 698, and 714 nm, respectively. The wavelengths of CP43, CP47, and PSI in *Chlorella* were 687, 699, and 722 nm, respectively. The PSI fluorescence intensity was determined by subtracting 0.2 × CP43 fluorescence intensity from the observed fluorescence intensity at the PSI peak (Yokono et al. 2015a). All values are the means ± SDs of three biological replicates. Individual values are based on Fig. 3

Fluorescence decay-associated spectra (FDAS)

To examine the net changes of amplitudes in steady-state fluorescence spectra, we measured TRFS and constructed FDAS through a global analysis of TRFS. Figure 4 shows the FDAS of *Chlamydomonas* and *Chlorella* on 459-nm excitation. To fit the fluorescence rise and decay curves in both green algae, six time constants were necessary: 25–30, 140–160, 700–860 ps, 1.9–2.2, 6.0–6.1, and 29–31 ns in *Chlamydomonas*, and 25–35, 140–170, 960–1000 ps, 2.5–2.6, 6.0–6.1, and 30–32 ns in *Chlorella*. FDAS were normalized to the integrated intensity of absolute steady-state fluorescence spectra (Fig. 3). Hence, the differences of amplitudes in FDAS reflect absolute intensity changes.

First, we discuss the changes of FDAS based on the results of the control cells shown in Fig. 4a. In the first FDAS, the positive band was observed below ~680 nm, while the negative bands were found at ~688 and ~710 nm in *Chlamydomonas* (~720 nm in *Chlorella*). These pairs of positive and negative bands indicate the energy transfer from LHC to both PSs (Włodarczyk et al. 2016). The negative bands were more enhanced in *Chlorella* compared with *Chlamydomonas*. In the second FDAS, there were two positive amplitudes at 686 and 710 nm. Previous studies have reported that the former mainly comes from trapping

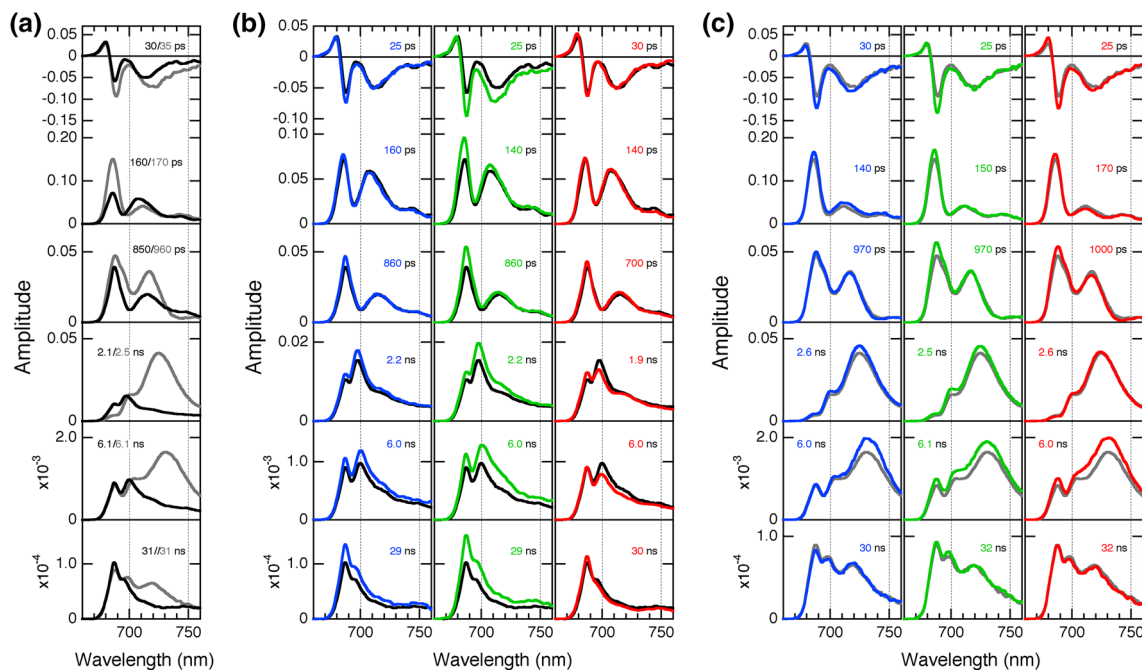


Fig. 4 Fluorescence decay-associated spectra (FDAS) of *Chlamydomonas* and *Chlorella* cells grown under different light qualities at 77 K: FDAS of *Chlamydomonas* (black) and *Chlorella* (gray) cells grown under white LEDs (a), FDAS of *Chlamydomonas* cells grown under monochromatic LEDs (b), and FDAS of *Chlorella* cells grown under monochromatic LEDs (c). The excitation wavelength was

459 nm. The amplitudes were normalized to the integrated intensity of steady-state fluorescence spectrum (Fig. 3). The blue, green, and red lines indicate the cells grown under blue, green, and red LEDs, respectively. The black and gray lines are FDAS of the control cells in b, c, respectively

at PSII RC (Caffarri et al. 2011), while the latter exhibits fluorescence from PSI red-Chl (Włodarczyk et al. 2015). The amplitude of the PSII band was twice as large in *Chlorella* than in *Chlamydomonas*, while the PSI band was more enhanced in *Chlamydomonas*. In the third FDAS, two peaks were observed around 688 and 715 nm. The wavelengths of the peaks were longer than those in the second FDAS, indicating the presence of another low-energy Chl. In the fourth FDAS, two clear bands around 685 and 695 nm and a shoulder at ~715 nm were observed in *Chlamydomonas*. In *Chlorella*, a clear PSI band was found with two other small bands in the PSII fluorescence region. These results suggest the presence of further lower-energy Chl. The amplitude of the ~695 nm band was coincident between both green algae, while the positive amplitude of PSI fluorescence was similar to those in the second and third FDAS in *Chlorella*, and the amplitude gradually decreased from the second to fourth FDAS in *Chlamydomonas*. The fifth FDAS exhibited fluorescence from the final acceptor of energy-transfer pathways. Since the final acceptor does not transfer energy to other pigments, the lifetime is similar to that of free Chl *a*. The amplitudes of the peak bands were very small compared with the sum of all amplitudes in the corresponding peaks. Therefore, the effect of this component on steady-state fluorescence appears to be limited. The sixth FDAS revealed delayed fluorescence (DF), which is thought to originate from charge recombination at PSII RC (Mimuro et al. 2007). DF was observed only in the PSII fluorescence region in *Chlamydomonas*, while *Chlorella* exhibited DF in both the PSII and PSI fluorescence regions. In addition, the CP47/CP43 intensity ratio in *Chlorella* was higher than that in *Chlamydomonas*.

Compared with W-grown cells, the monochromatic-LED grown cells exhibited large changes in energy-transfer processes (Fig. 4b, c). In the B-grown *Chlamydomonas* cells, the negative band in the first FDAS and the positive band in other FDAS were enhanced in the PSII fluorescence region. However, the increase of the positive band was smaller in the second FDAS than in the other FDAS. The G-grown *Chlamydomonas* cells exhibited increased negative amplitude in the first FDAS and increased positive amplitude in other FDAS in the PSII and PSI fluorescence regions. The amplitude of the PSII band increased and the time constant became shorter in the third FDAS of the R-grown *Chlamydomonas* cells. Moreover, the band around 695 nm was reduced in the fourth FDAS. In the DF spectra (the sixth FDAS), the monochromatic-LED grown *Chlamydomonas* cells showed no clear PSI fluorescence and the CP47/CP43 intensity ratio decreased only in the R-grown *Chlamydomonas* cells. Under a monochromatic LED, *Chlorella* exhibited enhanced negative amplitude in the first FDAS and positive amplitude in the other FDAS in the PSII fluorescence region. However, the increased positive amplitude

from the third FDAS to the second FDAS was smaller in the B-grown *Chlorella* cells than in the G- and R-grown *Chlorella* cells. In the PSI fluorescence region, the negative band in the first FDAS was enhanced under B- and R-LED conditions. The positive bands in the second and fourth FDAS were increased under B-LED, while the G-grown *Chlorella* cells exhibited enhanced bands in the fourth FDAS. The R-grown *Chlorella* cells exhibited decreased positive amplitudes in the second and third FDAS. In addition, the band at ~680 nm was increased under R-LED conditions. The PSI/PSII intensity ratio in the DF spectra (the sixth FDAS) of the monochromatic-LED grown *Chlorella* cells was similar to that of the control cells.

Discussion

Differences of light-harvesting and energy-transfer processes between two unicellular green algae

Green algae contain Chl *a*, Chl *b*, and Car as photosynthetic pigments. A previous study reported that synthesized Car was no different between *Chlamydomonas* and *Chlorella* (Kunugi et al. 2016). However, the absorption spectra of the control cells were different (Fig. 2). In *Chlamydomonas* and *Chlorella*, only LHCs contain Chl *b* (Kunugi et al. 2016). Therefore, the Chl *b*/chl *a* ratio in an absorption spectrum corresponds to the relative amount of LHC to PS. In the current study, we found that the ratio was larger in *Chlamydomonas* than in *Chlorella* (Fig. 2; Table 1), indicating that *Chlamydomonas* exhibited a larger LHC/PS ratio. In the 450–500 nm region of the absorption spectra, *Chlamydomonas* and *Chlorella* exhibited one band and two bands, respectively (Fig. 2). These differences could originate from the relative amount of LHC to PS and the composition of Car. Thus, light-harvesting ability appeared to differ between the two green algae grown under W-LED.

In addition to light-harvesting ability, energy-transfer processes also differed between the two green algae (Fig. 4a). The negative bands were more enhanced in *Chlorella* compared with *Chlamydomonas* (the first FDAS), indicating that more energy was transferred from LHCs to PSs in *Chlorella*. In the DF spectra, clear PSI fluorescence was observed in *Chlorella* but not in *Chlamydomonas* (the sixth FDAS). These results indicate that spillover occurs in *Chlorella*, whereas the contribution was particularly small in *Chlamydomonas*, as observed in a land plant *Arabidopsis thaliana* (Yokono et al. 2015a). Moreover, in the sixth FDAS, the CP47/CP43 intensity ratio was larger in *Chlorella* than in *Chlamydomonas*, indicating that more energy was transferred between the neighboring PSII monomers in *Chlorella*, as observed in diatoms (Yokono et al. 2015b). The largest difference was the magnitude of positive amplitude in the

second FDAS assigned to the trapping of PSII, suggesting that *Chlorella* uses light energy more efficiently than *Chlamydomonas*. In the PSI fluorescence region, *Chlorella* exhibited similar amplitude in the second to fourth FDAS, while the amplitudes gradually decreased from the second to fourth FDAS in *Chlamydomonas*. These differences appear to come from the energy-transfer pathways from LHCs to PSI. However, in the case of *Chlorella*, the energy-transfer pathways via spillover could also contribute to the differences.

Regulation of light-harvesting and energy-transfer processes under different light qualities

Compared with W-grown cells, the monochromatic-LED grown cells exhibited modified light-harvesting and energy-transfer processes (Figs. 2, 3, 4). Under different light qualities, cyanobacteria and red algae have been reported to regulate the contribution of spillover, and to change the PSI/PSII intensity ratio in DF (Akimoto et al. 2012, 2013; Ueno et al. 2015). However, neither of the green algae examined in the current study showed a clear change in the intensity ratio (the sixth FDAS in Fig. 4b, c). The responses of these green algae are similar to the previously reported responses of cyanobacterium *Prochlorococcus*, which possesses unique antenna Pcb containing both Chl *a*- and Chl *b*-type Chls, but not PBS (Hamada et al. 2017). It has been suggested that *Prochlorococcus* controls its light-harvesting antennas with a small modification of both PSs in response to light conditions (Hamada et al. 2017). Therefore, two unicellular green algae could regulate the associations between LHCs and PSs under different light qualities.

B-LED is mainly absorbed by Chl *b* (see Fig. 1), causing PSII excitation. Both the unicellular green algae cells grown under B-LED exhibited different changes of the Chl *b*/Chl *a* ratio (Fig. 2; Table 1). This difference might originate from the LHC/PS ratio under W-LED conditions (Fig. 2; Table 1). However, compared with the change of the PBS/Chl *a* ratio observed in cyanobacteria and red algae (Ghosh and Govindjee 1966; Myers et al. 1980; Ley and Butler 1980; Manodori and Melis 1986; Cunningham et al. 1990; Akimoto et al. 2012, 2013; Ueno et al. 2015), the change of the Chl *b*/Chl *a* ratio in the current study was negligibly small. Both the B-grown *Chlamydomonas* and *Chlorella* cells exhibited enhanced negative amplitude in the first FDAS and positive amplitude in other FDAS in the PSII fluorescence region (Fig. 4b, c), indicating an increase of energy transfer from LHCII to PSII. However, in *Chlamydomonas*, the increase of amplitude in the second FDAS was smaller than that in the third and fourth FDAS. This result suggests that more energy is transferred from LHCII to Chl located in the distant place of PSII RC. On the other hand, *Chlorella* exhibited a smaller increase of amplitude in the third FDAS than in the second and

fourth FDAS, suggesting that more energy transferred to PSII, but part of the energy flowed to lowest-energy Chl within PSII. Car is reported to be present near the lowest-energy Chl of CP47, and may function as a quencher (Groot et al. 1995; Andrizhiyevskaya et al. 2005). Moreover, in the B-grown *Chlorella* cells, the positive bands in the second and fourth FDAS increase with the enhancement of the negative band in the first FDAS in the PSII fluorescence region. This result indicates that energy is transferred from LHC to PSI through different energy-transfer pathways. Direct energy transfer from LHC to PSI is one of the pathways to PSI. However, in the B-grown *Chlorella* cells, spillover occurred (the sixth FDAS in Fig. 4c) with an accompanying increase of energy transfer to PSII. Hence, energy transfer from LHCII to PSI via spillover may provide another pathway to PSI.

G-LED is mainly absorbed by Car (see Fig. 1), which functions as both a sensitizer and quencher. Green algae containing siphonaxanthin utilize green light for photosynthesis because siphonaxanthin efficiently transfers energy to Chl *a* (Akimoto et al. 2004, 2007). However, the green algae used in this study do not contain siphonaxanthin (Kunugi et al. 2016). G-grown *Chlamydomonas* and *Chlorella* cells showed a different change of the Chl *b*/Chl *a* ratio (Fig. 2; Table 1), but the change was small, and similar to that of the B-grown cells. The G-grown *Chlamydomonas* cells exhibited enhanced negative bands in the first FDAS and positive bands in other FDAS (Fig. 4b). This result indicates that *Chlamydomonas* exhibited increased energy transfer from LHCs to PSs under G-LED. In contrast, G-grown *Chlorella* cells exhibited increased negative amplitude in the first FDAS and positive bands in other FDAS in the PSII fluorescence region (Fig. 4c), reflecting the enhancement of energy transfer from LHCII to PSII. The changes in the magnitudes of the negative bands (the first FDAS in Fig. 4b, c) were larger than those of the Chl *b*/Chl *a* ratio in the absorption spectra (Fig. 2; Table 1), suggesting that LHCs may have switched from a “quenching” mode to a “light-harvesting” mode in both green algae (Ruban et al. 2012; Ballottari et al. 2014). In the PSI fluorescence region of *Chlorella*, the amplitudes of positive bands in the fourth FDAS increased, although those of the negative bands in the first FDAS did not change. As mentioned above, the current results revealed that spillover occurred in *Chlorella* (the sixth FDAS in Fig. 4c). Since the peak wavelength of PSI fluorescence in DF was between the PSI peaks in the third and fourth FDAS, the spillover contributed to both red-Chl. Therefore, *Chlorella* appears to transfer more energy from LHCII to PSI via spillover, modifying the direct energy-transfer pathways from LHC to PSI under G-LED. Thus, both the unicellular green algae under G-LED cultivation exhibited an increase in steady-state fluorescence of PSII and PSI (Fig. 3), but the origins of these changes were different.

R-LED is mainly absorbed by Chl *a* (see Fig. 1) and excites PSII. Under R-LED, both green algae exhibited decreased Chl *b*/Chl *a* ratios (Fig. 2; Table 1), in accord with the findings of previous studies (Kowallik and Schürmann 1984; Humbeck et al. 1988; Melis et al. 1996). In the PSII fluorescence region of R-grown *Chlorella* cells, the negative peak in the first FDAS and the positive peaks in the second and third FDAS were enhanced (Fig. 4c). This result indicates increased energy transfer from LHCII to PSII. However, since the amplitudes around 695 nm were similar to those in the control cells, the results suggested that energy transfer to the lowest-energy Chl within PSII was suppressed. The negative band in the PSI fluorescence region was reduced (the first FDAS in Fig. 4c), indicating the enhancement of direct energy transfer from LHC to PSI. Nevertheless, the positive bands decreased in the second and third FDAS, and did not change in the fourth FDAS. In the case of *Chlorella*, not only direct energy transfer from LHC to PSI but also energy transfer from LHCII to PSI via spillover (see the sixth FDAS in Fig. 4c) contributes to PSI bands. The increase of positive amplitude around 680 nm comes from quenching within LHC. Therefore, it is considered that energy transfer from LHCII to PSI via spillover is reduced by quenching, and moreover, direct energy-transfer pathways from LHC to PSI are modified under R-LED conditions. The lower CP47/CP43 intensity ratio in the DF spectra of the R-grown *Chlamydomonas* cells indicates the suppression of energy transfer between neighboring PSII monomers under R-LED. Moreover, the time constant was largely reduced in the third FDAS and the amplitude of the CP47 band decreased in the fourth FDAS (Fig. 4b), suggesting that fluorescence quenching might be induced within PSs. The cation form of Chl_Z (Mohamed et al. 2016) and Car located near the lowest-energy Chl (Groot et al. 1995; Andrizhiyevskaya et al. 2005) within PSII, and the oxidized PSI RC (Schlodder et al. 2011) are potential candidates for quenching. A previous study of *Chlamydomonas* reported that light-harvesting complex stress-related (LHCSR) proteins function as quenchers in green algae (Peers et al. 2009). However, the contribution of proteins is unlikely in the current study because the light intensity for cultivation (50 μmol photons m⁻² s⁻¹) was too low to accumulate LHCSR proteins (Tokutsu and Minagawa 2013; Dinc et al. 2016; Kim et al. 2017), and R-LED does not induce the accumulation of LHCSR proteins (Allorent et al. 2016; Petroustos et al. 2016).

Summary

In the current study, we examined the light-harvesting function of two kinds of unicellular green algae *Chlamydomonas* and *Chlorella* cells grown under various light qualities by constructing absolute intensity FDAS from the combination

of absolute steady-state fluorescence spectra and TRFS. By observing the DF spectra (the sixth FDAS in Fig. 4), we demonstrated that both types of unicellular green algae regulate the interactions between LHCs and PSs. B-grown *Chlamydomonas* cells transferred more energy from LHCII to low-energy Chl located far from PSII RC (the second to fourth FDAS in Fig. 4b). In B-grown *Chlorella* cells, the energy transferred from LHCII mainly flowed to the lowest-energy Chl of CP47 (the second to fourth FDAS in Fig. 4c). Moreover, more energy transferred to PSI by direct energy transfer from LHC to PSI and energy transfer from LHCII to PSI via spillover (the second, fourth, and sixth FDAS in Fig. 4c). Under G-LED, LHC changed to “light-harvesting” mode to increase light-harvesting ability (Figs. 2, 4); *Chlamydomonas* exhibited enhanced energy transfer from LHCs to PSs, while *Chlorella* exhibited increased energy transfer from LHCII to PSII, but some of the energy was transferred to PSI via spillover (the fourth FDAS in Fig. 4). R-grown *Chlamydomonas* cells suppressed energy transfer between the neighboring PSII monomers PSII (the sixth FDAS in Fig. 4b). In addition, quenching occurred within PSs (the third and fourth FDAS in Fig. 4b). Under R-LED, *Chlorella* exhibited increased energy transfer from LHCs to PSs (the first FDAS in Fig. 4c) and suppressed energy transfer to the lowest-energy Chl within PSII (the fourth FDAS in Fig. 4c). Moreover, energy transfer from LHCII to PSI via spillover was decreased by quenching within LHCs (the first FDAS in Fig. 4c). Thus, spillover may play an important role in balancing excitation between PSII and PSI in *Chlorella*.

Acknowledgements This work was supported in part by Special Coordination Funds for promoting Science and Technology, Creation of Innovation Centers for Advanced Interdisciplinary Research Areas (Innovative Bioproduction, Kobe), Japan, and by JSPS KAKENHI (Grant No. 16H06553 to S.A.). We thank Benjamin Knight, MSc., from Edanz Group (<http://www.edanzediting.com/ac>) for editing a draft of this manuscript.

References

- Aizawa K, Shimizu T, Hiyama T, Satoh K, Nakamura Y, Fujita Y (1992) Changes in composition of membrane proteins accompanying the regulation of PSI/PSII stoichiometry observed with *Synechocystis* PCC 6803. *Photosynth Res* 32:131–138
- Akimoto S, Yamazaki I, Murakami A, Takaichi S, Mimuro M (2004) Ultrafast excitation relaxation dynamics and energy transfer in the siphonaxanthin-containing green alga *Codium fragile*. *Chem Phys Lett* 390:45–49
- Akimoto S, Tomo T, Naitoh Y, Otomo A, Murakami A, Mimuro M (2007) Identification of a new excited state responsible for the in vivo unique absorption band of siphonaxanthin in the green alga *Codium fragile*. *J Phys Chem B* 111:9179–9181
- Akimoto S, Yokono M, Hamada F, Teshigahara A, Aikawa S, Kondo A (2012) Adaptation of light-harvesting systems of *Arthrospira platensis* to light conditions, probed by time-resolved fluorescence spectroscopy. *Biochim Biophys Acta Bioenerg* 1817:1483–1489

- Akimoto S, Yokono M, Aikawa S, Kondo A (2013) Modification of energy-transfer processes in the cyanobacterium, *Arthrospira platensis*, to adapt to light conditions, probed by time-resolved fluorescence spectroscopy. *Photosynth Res* 117:235–243
- Allorent G, Lefebvre-Legendre L, Chappuis R, Kuntz M, Truong TB, Niyogi KK, Ulm R, Goldschmidt-Clermont M (2016) UV-B photoreceptor-mediated protection of the photosynthetic machinery in *Chlamydomonas reinhardtii*. *Proc Natl Acad Sci USA* 113:14864–14869
- Andrizhiyevskaya EG, Chojnicka A, Bautista JA, Diner BA, van Grondelle R, Dekker JP (2005) Origin of the F685 and F695 fluorescence in photosystem II. *Photosynth Res* 84:173–180
- Ballottari M, Alcocer MJP, D'Andrea C, Viola D, Ahn TK, Petrozza A, Polli D, Fleming GR, Cerullo G, Bassi R (2014) Regulation of photosystem I light harvesting by zeaxanthin. *Proc Natl Acad Sci USA* 111:E2431–E2438
- Blankenship RE (2014) Molecular mechanisms of photosynthesis, 2nd edn. Wiley-Blackwell, Hoboken
- Caffarri S, Broess K, Croce R, van Amerongen H (2011) Excitation energy transfer and trapping in higher plant Photosystem II complexes with different antenna sizes. *Biophys J* 100:2094–2103
- Chen HB, Wu JY, Wang CF, Fu CC, Shieh CJ, Chen CI, Wang CY, Liu YC (2010) Modeling on chlorophyll a and phycocyanin production by *Spirulina platensis* under various light-emitting diodes. *Biochem Eng J* 53:52–56
- Chow WS, Melis A, Anderson JM (1990) Adjustments of photosystem stoichiometry in chloroplasts improve the quantum efficiency of photosynthesis. *Proc Natl Acad Sci USA* 87:7502–7506
- Cunningham FX Jr, Dennenberg RJ, Jursinic PA, Gantt E (1990) Growth under red light enhances photosystem II relative to photosystem I and phycobilisomes in the red alga *Porphyridium cruentum*. *Plant Physiol* 93:888–895
- Dinc E, Tian L, Roy LM, Roth R, Goodenough U, Croce R (2016) LHCSR1 induces a fast and reversible pH-dependent fluorescence quenching in LHClI in *Chlamydomonas reinhardtii* cells. *Proc Natl Acad Sci USA* 113:7673–7678
- Gantt E (1981) Phycobilisomes. *Annu Rev Plant Physiol* 32:327–347
- Garnier J, Maroc J, Guyon D (1986) Low-temperature fluorescence emission spectra and chlorophyll-protein complexes in mutants of *Chlamydomonas reinhardtii*: evidence for a new chlorophyll-a-protein complex related to Photosystem I. *Biochim Biophys Acta Bioenerg* 851:395–406
- Ghosh AK, Govindjee (1966) Transfer of the excitation energy in *Anacystis nidulans* grown to obtain different pigment ratios. *Biophys J* 6:611–619
- Groot ML, Peterman EJG, van Stokkum IHM, Dekker JP, van Grondelle R (1995) Triplet and fluorescing states of the CP47 antenna complex of photosystem II studied as a function of temperature. *Biophys J* 68:281–290
- Hamada F, Murakami A, Akimoto S (2017) Adaptation of divinyl chlorophyll *alb*-containing cyanobacterium to different light conditions: Three strains of *Prochlorococcus marinus*. *J Phys Chem B* 121:9081–9090
- Humbeck K, Hoffmann B, Senger H (1988) Influence of energy flux and quality of light on the molecular organization of the photosynthetic apparatus in *Scenedesmus*. *Planta* 173:205–212
- Ichimura T (1971) Sexual cell division and conjugation-papilla formation in sexual reproduction of *Closterium strigosum*. In: Nishizawa K (ed) Proceedings of the 7th international seaweed symposium, University of Tokyo Press, Tokyo, pp 208–214
- Ihalainen JA, van Stokkum IHM, Gibasiewicz K, Germano M, van Grondelle R, Dekker JP (2005) Kinetics of excitation trapping in intact photosystem I of *Chlamydomonas reinhardtii* and *Arabidopsis thaliana*. *Biochim Biophys Acta Bioenerg* 1706:267–275
- Kim E, Akimoto S, Tokutsu R, Yokono M, Minagawa J (2017) Fluorescence lifetime analyses reveal how the high light-responsive protein LHCSR3 transforms PSII light-harvesting complexes into an energy-dissipative state. *J Biol Chem* 292:18951–18960
- Kowallik W, Schürmann R (1984) Chlorophyll *a*/Chlorophyll *b* ratios of *Chlorella vulgaris* in blue or red light. In: Senger H (ed) Blue light effects in biological systems. Springer, Berlin/Heidelberg, pp 352–358
- Kunugi M, Satoh S, Ihara K, Shibata K, Yamagishi Y, Kogame K, Obokata J, Takabayashi A, Tanaka A (2016) Evolution of green plants accompanied changes in light-harvesting systems. *Plant Cell Physiol* 57:1231–1243
- Ley AC, Butler WL (1980) Effects of chromatic adaptation on the photochemical apparatus of photosynthesis in *Porphyridium cruentum*. *Plant Physiol* 65:714–722
- Liu Z, Yan H, Wang K, Kuang T, Zhang J, Gui L, An X, Chang W (2004) Crystal structure of spinach major light-harvesting complex at 2.72 Å resolution. *Nature* 428:287–292
- Manodori A, Melis A (1986) Cyanobacterial acclimation to PSI or PSII light. *Plant Physiol* 82:185–189
- Markou G (2014) Effect of various colors of light-emitting diode (LEDs) on the biomass composition of *Arthrospira platensis* cultivated in semi-continuous mode. *Appl Biochem Biotechnol* 172:2758–2768
- Melis A, Harvey GW (1981) Regulation of photosystem stoichiometry, chlorophyll *a* and chlorophyll *b* content and relation to chloroplast ultrastructure. *Biochim Biophys Acta Bioenerg* 637:138–145
- Melis A, Murakami A, Nemson JA, Aizawa K, Ohki K, Fujita Y (1996) Chromatic regulation in *Chlamydomonas reinhardtii* alters photosystem stoichiometry and improves the quantum efficiency of photosynthesis. *Photosynth Res* 47:253–265
- Mimuro M, Akimoto S, Tomo T, Yokono M, Miyashita H, Tsuchiya T (2007) Delayed fluorescence observed in the nanosecond time region at 77 K originates directly from the photosystem II reaction center. *Biochim Biophys Acta Bioenerg* 1767:327–334
- Mirkovic T, Ostroumov EE, Anna JM, van Grondelle R, Govindjee, Scholes GD (2017) Light absorption and energy transfer in the antenna complexes of photosynthetic organisms. *Chem Rev* 117:249–293
- Mohamed A, Nagao R, Noguchi T, Fukumura H, Shibata Y (2016) Structure-based modeling of fluorescence kinetics of photosystem II: relation between its dimeric form and photoregulation. *J Phys Chem B* 120:365–376
- Murakami A (1997) Quantitative analysis of 77K fluorescence emission spectra in *Synechocystis* sp. PCC 6714 and *Chlamydomonas reinhardtii* with variable PSI/PSII stoichiometries. *Photosynth Res* 53:141–148
- Myers J, Graham JR, Wang RT (1980) Light harvesting in *Anacystis nidulans* studied in pigment mutants. *Plant Physiol* 66:1144–1149
- Peers G, Truong TB, Ostendorf E, Busch A, Elrad D, Grossman AR, Hippler M, Niyogi KK (2009) An ancient light-harvesting protein is critical for the regulation of algal photosynthesis. *Nature* 462:518–521
- Petroutsos D, Tokutsu R, Maruyama S, Flori S, Greiner A, Magneschi L, Cusant L, Kottke T, Mittag M, Hegemann P, Finazzi G, Minagawa J (2016) A blue-light photoreceptor mediates the feedback regulation of photosynthesis. *Nature* 537:563–566
- Ruban AV, Johnson MP, Duffy CDP (2012) The photoprotective molecular switch in the photosystem II antenna. *Biochim Biophys Acta Bioenerg* 1817:167–181
- Schlodder E, Hussels M, Cetin M, Karapetyan NV, Brecht M (2011) Fluorescence of the various red antenna states in photosystem I complexes from cyanobacteria is affected differently by the redox state of P700. *Biochim Biophys Acta Bioenerg* 1807:1423–1431
- Shibata Y, Nishi S, Kawakami K, Shen JR, Renger T (2013) Photosystem II does not possess a simple excitation energy funnel: time-resolved fluorescence spectroscopy meets theory. *J Am Chem Soc* 135:6903–6914

- Sueoka N (1960) Mitotic replication of deoxyribonucleic acid in *Chlamydomonas reinhardtii*. Proc Natl Acad Sci USA 46:83–91
- Tokutsu R, Minagawa J (2013) Energy-dissipative supercomplex of photosystem II associated with LHCSR3 in *Chlamydomonas reinhardtii*. Proc Natl Acad Sci USA 110:10016–10021
- Ueno Y, Aikawa S, Kondo A, Akimoto S (2015) Light adaptation of the unicellular red alga *Cyanidioschyzon merolae*, probed by time-resolved fluorescence spectroscopy. Photosynth Res 125:211–218
- Ueno Y, Shimakawa G, Miyake C, Akimoto S (2018) Light-harvesting strategy during CO₂-dependent photosynthesis in the green alga *Chlamydomonas reinhardtii*. J Phys Chem Lett 9:1028–1033
- Wlodarczyk LM, Snellenburg JJ, Ihalainen JA, van Grondelle R, van Stokkum IHM, Dekker JP (2015) Functional rearrangement of the light-harvesting antenna upon state transitions in a green alga. Biophys J 108:261–271
- Wlodarczyk LM, Dinc E, Croce R, Dekker JP (2016) Excitation energy transfer in *Chlamydomonas reinhardtii* deficient in the PSI core or the PSII core under conditions mimicking state transitions. Biochim Biophys Acta Bioenerg 1857:625–633
- Yokono M, Takabayashi A, Akimoto S, Tanaka A (2015a) A megacomplex composed of both photosystem reaction centres in higher plants. Nat Commun 6:6675
- Yokono M, Nagao R, Tomo T, Akimoto S (2015b) Regulation of excitation energy transfer in diatom PSII dimer: how does it change the destination of excitation energy? Biochim Biophys Acta Bioenerg 1847:1274–1282